MICROSCOPIC SURFACE CHARACTERIZATION OF TECHNICAL AND TEXTILE POLYACRYLONITRILE FIBERS

Christina Kunzmann[1], Tobias Peter[1], Judith Moosburger-Will[2] and Siegfried Horn[1,2]

[1]Institute of Physics, Experimental Physics II, University of Augsburg, 86135 Augsburg, Germany
Email: Christina.Kunzmann@physik.uni-augsburg.de,
Web Page: http:// www.physik.uni-augsburg.de/exp2
[2]Institute of Materials Resource Management, University of Augsburg, 86135 Augsburg, Germany
Web Page: http://www.mrm.uni-augsburg.de

Keywords: PAN, AFM, surface structure, nanopores

Abstract
In our study we present an investigation of the surfaces of two technical and one textile polyacrylonitrile (PAN) fibers on nanoscale by atomic force microscopy (AFM) utilizing a super sharp tip with a tip radius of about 2 nm. Before analysis, the finish of the fibers was removed. The AFM analysis of all three PAN fiber surfaces shows a fibrillar structure with fibril orientation along the fiber axis. Additionally, the existence of a surface porosity on the nanoscale is observed. These nanostructures are detected on both technical as well as on the textile PAN fibers and are distributed homogenously over the surface of the fibers. While the nanopores of the two technical PAN fibers show a size of about 12 nm, the textile fibers have larger pore size of about 22 nm. In addition, the three PAN fibers vary in the orientation of the pores along the fiber axis. The AFM results are correlated to effective surface areas from the Brunauer-Emmett-Teller gas adsorption and to crystalline parameters from X-ray diffraction measurements.

1. Introduction

Polyacrylonitrile (PAN) is a semicrystalline thermoplast, which is used for a variety of products, e.g. membranes, hollow fibers for osmosis, textiles, or as precursor material for carbon fiber production. [1, 1, 2] PAN fibers are produced using a dry jet or wet spinning process [3]; the latter is the common production method for manufacturing of tows with a large number of filaments. In the wet spinning process a PAN solution is spun through a spinneret into a coagulation bath. [4–7] After immersion in the nonsolvent coagulation bath, the solution becomes thermodynamically unstable and spinodal decomposition in two phases occurs. [5, 8, 9] A polymer-rich phase forms the bulk of the fiber, while a solvent-rich phase forms voids. [5, 10, 8] This structure is called gel network. [9] It was shown that the shell of such fibers is porous and the pore size depends on the conditions of the coagulation. [8, 7, 11] After the coagulation, the fibers undergo repeated steps of washing and stretching. Stretching is an important step to orientate the molecules and influences the properties of the fibers. [12, 13] Finally, a polymeric finish which acts as antistatic and lubricant is applied to ease handling and to protect the fibers in the following steps of the process chain. [4, 13, 14]

PAN fibers are the most important precursor material for carbon fiber production. [15, 16] Due to the increasing field of applications of carbon fiber reinforced composite materials, the demand for carbon

Excerpt from ISBN 978-3-00-053387-7

fibers is growing. [17–19] In the last decades the PAN fiber has been developed and optimized for this technical application because the quality of carbon fibers is closely linked to the properties of precursor fibers. Therefore, comprehensive knowledge of the precursor fiber chemistry and microstructure is important. Investigation of the evolution of the surface microstructure along the production process is one approach to obtain a fundamental understanding of process induced structural changes.

The atomic force microscopy (AFM) technique allows to investigate the surface topography of carbon fibers as well as non-conducting PAN fibers. [20] AFM permits a non-destructive characterization of the surface morphology and allows collection of quantitative lateral and height information on a nanoscale. The lateral resolution sensitively depends on the geometry and durability of the tip used. In recent years newly developed technologies enable the production of tips with high aspect ratio and small diameter. Such tips allow precise measurements of nanoscale structures.

2. Experimental

In the present work technical PAN fibers (PAN 1 and PAN 2) and textile PAN fibers (PAN 3) were analyzed. The fibers are equipped with different types of finish of unknown chemical composition. To analyze the surface of the fibers on nanoscale the finishes of the fibers have to be removed. For the desizing procedure different solvents were used, namely 0.1 M/L solution of Tetrabutylammonium fluoride trihydrate (TBAF, ACROS organics, 90 %) in Tetrahydrofuran (THF, Sigma Aldrich, ≥ 99.9%), 2-Butanon (MEK, Carl Roth GmbH + Co. KG, ≥ 99.5 %) and distillated water with curd soap (ISANA, Rossmann GmbH). The chemical composition of the cleaned fiber surfaces was controlled by X-ray photoelectron spectroscopy (XPS) using an Omicron XM 1000 electron analyzer with a monochromatized X-ray Al Kα source.

The AFM measurements on the fibers were performed using a Bruker Dimension ICON in tapping mode with super sharp EBD-SSS NCHR AFM probes from Nanotools with a tip radius of 2 nm. The scanning area of the images was 500nm x 500nm (512 x 512 pixels). The images were processed using the software Nanoscope Analysis v1.40. The fiber axis is marked in all figures with white arrows. The Brunauer-Emmett-Teller (BET) gas adsorption investigations were executed using an Autosorb iQ with Krypton as analysis gas. X-ray diffraction (XRD) investigations were operated at a Seifert 3003 PTS XRD diffractometer with a copper anode. The crystallinity and orientation of the crystallites were determined according to Ref. [21].

3. Results and discussions

3.1 Desizing of PAN fibers

Figure 2 (a, b) shows the AFM height and phase images of a technical PAN fiber (PAN 1). This fiber surface is covered with a technical finish. Both images height (a) and phase (b) show a fibrillar structure of the fiber along the fiber axis. In addition, a nanoscale fine structure is faintly visible, similar to that observed on carbon fiber surfaces. [22] In order to expose the nanostructured surface, the finish of the fibers was removed.

Excerpt from ISBN 978-3-00-053387-7

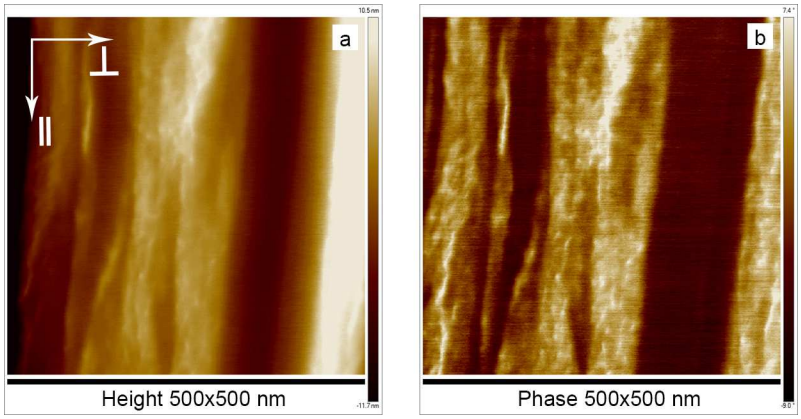

Figure 1. AFM height (a) and phase (b) image of the surface of a technical PAN fiber with textile finish.

Different commercial solvents were used to dissolve the finishes of unknown chemical composition from the PAN fibers. The desizing was controlled by XPS measurements monitoring oxygen and/or silicon concentration. The cleaning procedure was continued until the elemental composition of the fiber surface remained unchanged and AFM measurements showed a pronounced surface structure. The parameters of the most successful dissolving processes, i.e. the used solvent, temperature and time, for the different PAN fibers are listed in Table 1. The finish of all three fiber types can be removed in polar solvents. The silicon containing finish of the technical fiber PAN 1 can be effectively removed by a TBAF-THF solution. The best result of desizing the technical fiber PAN 2, which is equipped with a non-silicon containing finish, was achieved using MEK. In contrast, the non-silicon containing sizing of typical textile fibers like PAN 3 is dissolved in hot soap-water. All types of fibers were washed with 2-Propanol and water after the solvent treatment and dried at 40 °C for 8h before they were prepared for AFM analysis.

Table 1. Parameters of desizing treatment of PAN fibers.

Specimen Type	Solvent	*t* (min)	*T* (°C)
PAN 1	THF + TBAF	1080	20
PAN 2	MEK	300	20
PAN 3	H_2O + RCOONa	300	98

3.2 AFM investigation on nanoscale of PAN fiber surfaces

3.2.1 Nanostructures on technical PAN 1 fiber surface

Figure 2 (a) shows an AFM height image of size 5µm x 5µm of the technical fiber PAN 1 after the desizing procedure. The surface of the fibers consists of fibrils which are oriented parallel to the fiber axis and have an average width (perpendicular to fiber axis) of 180 ± 48 nm. In addition, a nanoscale structure is detected on the whole fiber surface. Small nanopores with an average width (perpendicular to fiber axis) of 11.7 ± 3.0 nm and an average length (parallel to fiber axis) of 15.7 ± 7.7 nm are found, which form chain like structure oriented along the fiber axis. Their depth amounts to 2.4 ± 1.1 nm and they are separated by thin intersections with an average width of 3.3 ± 2.1 nm. Often pores are observed which appear to result from a coalescence process of neighboring pores. The coalescing occurs between neighboring pores of a chain. The fact, that the pores are extended in fiber direction

Excerpt from ISBN 978-3-00-053387-7

and also coalescing occurs can be explained by the stretching treatment of the fibers during the PAN fiber production process described in literature. [23, 24]

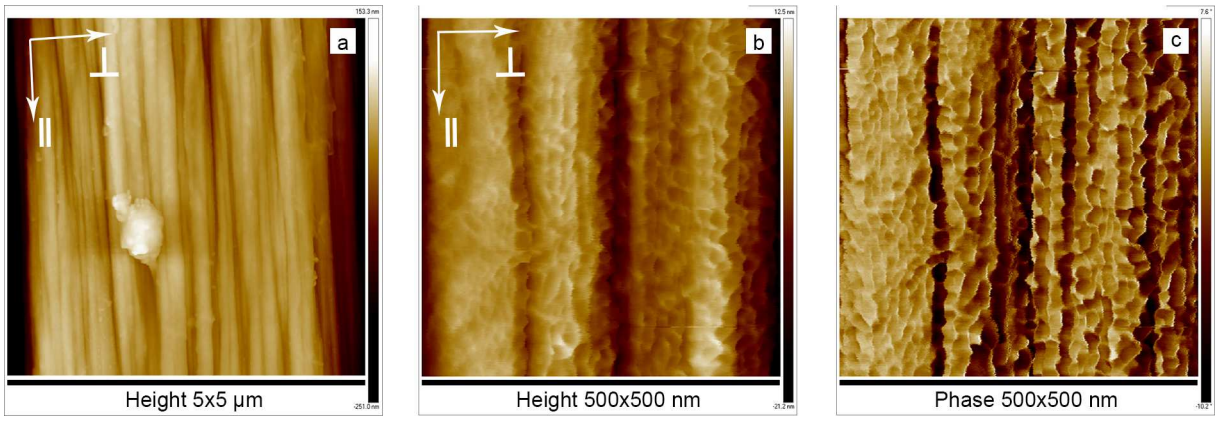

Figure 2. AFM height image (a) of size 5x5 µm and height (b) and phase (c) images of size 500x500 nm of the surface of a technical PAN fiber (PAN 1) after dissolving the finish.

For comparison, the surface of the corresponding carbon fiber (CF) is shown in Figure 3. This CF is produced from the PAN 1 fiber (equipped with silicon containing finish), and was taken out of the carbon fiber production process directly after carbonization i.e. before surface treatment by anodic oxidation and sizing. It was shown by XPS that the silicon-containing finish of PAN 1 is removed completely by the thermal treatment of the carbonization steps in the high temperature furnace. The CF shows a similar nanoporous surface structure, i.e. pores with an average width of 12.8 ±3.1 nm and an average length of 19.3 ± 8.5 nm. The comparison between PAN and carbon fiber suggests strongly that the nanostructures observed on the PAN fiber are characteristic for both fibers and, in particular, are no artifact created by removing the PAN fiber finish.

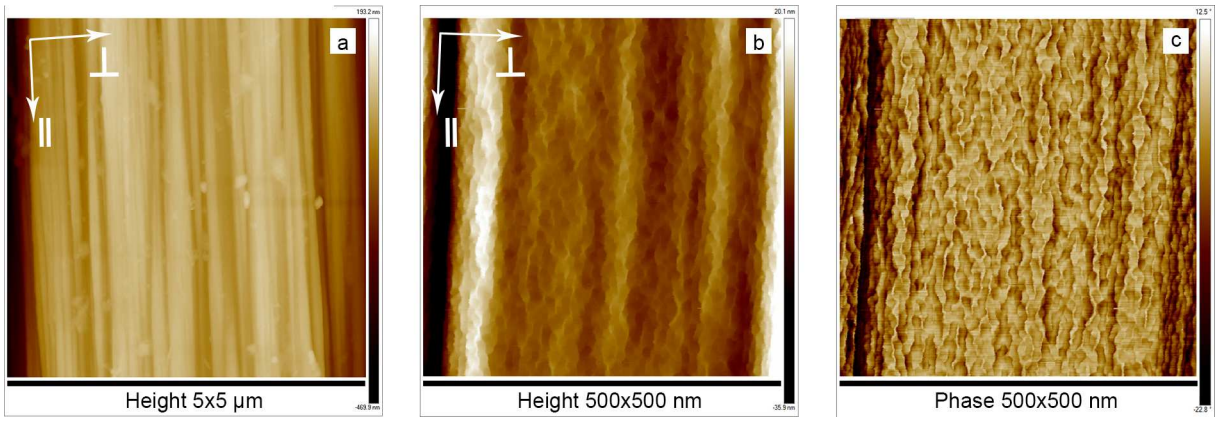

Figure 3. AFM height image (a) of size 5µm x 5µm and height (b) and phase (c) images of size 500x500 nm of carbon fiber CF surface.

3.2.2 Nanostructures on technical PAN 2 fiber surface

We additionally analyzed the desized surface of the second type of technical PAN fibers (PAN 2) on nanoscale. PAN 2 is precursor for carbon fibers with lower tensile strength than carbon fibers produced from PAN 1. These PAN 2 fibers also show a fibrillar structure (see Fig. 4a), with a fibril width of 589 ± 275 nm. The surface reveals also a nanoporous structure, as shown in the AFM height

Excerpt from ISBN 978-3-00-053387-7

and phase images in Fig. 4b and c. The pores have a similar size compared to that of PAN 1, with an average width of 11.1 ± 2.4 nm and a length of 19.7 ± 10.2 nm. The pores have a depth of about 2.3 ± 1.2 nm and are separated by intersections of 4.4 ± 1.7 nm width. In contrast to PAN 1 the pores of PAN 2 are less orientated along the fiber axis. Again, coalesced pores are detected, but in contrast to PAN 1, the resulting structures are not strictly aligned along the fiber axis.

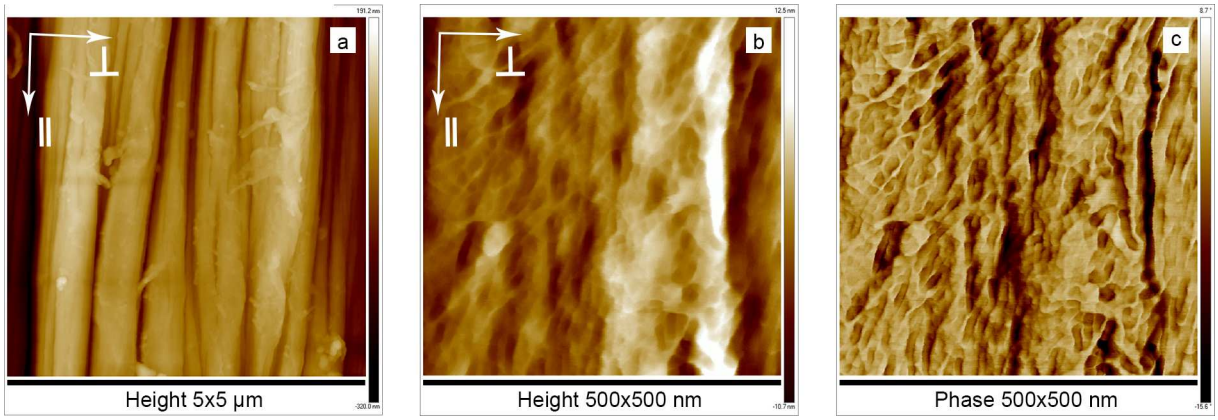

Figure 4. AFM height image (a) of 5x5 µm and height (b) and phase (c) images of the surface of PAN 2 after dissolving the finish.

3.2.3 Nanostructures on textile PAN 3 fiber surface

In Figure 5 the AFM images of the surface of a textile PAN fiber are shown. Again the surface reveals a fibrillar structure with a fibril width of 591 ± 261 nm (see Fig. 5 a). The image section of 500x500 surface of PAN 3 also shows the nanoscale structure already described above. These nanopores have an average depth of 2.1 ± 1.1 nm and an intersection width of 4.3 ± 2.7 nm, similar to those of the technical fibers. However, the average width of the pores is 22.2 ± 5.5 nm and the length is 23.0 ± 11.0 nm, which is clearly higher than the values of the technical PAN fibers. In contrast to the technical fibers, the majority of pores is not arranged in chains orientated along the fiber axis. Also pores, which are coalesced, have not a preferred orientation.

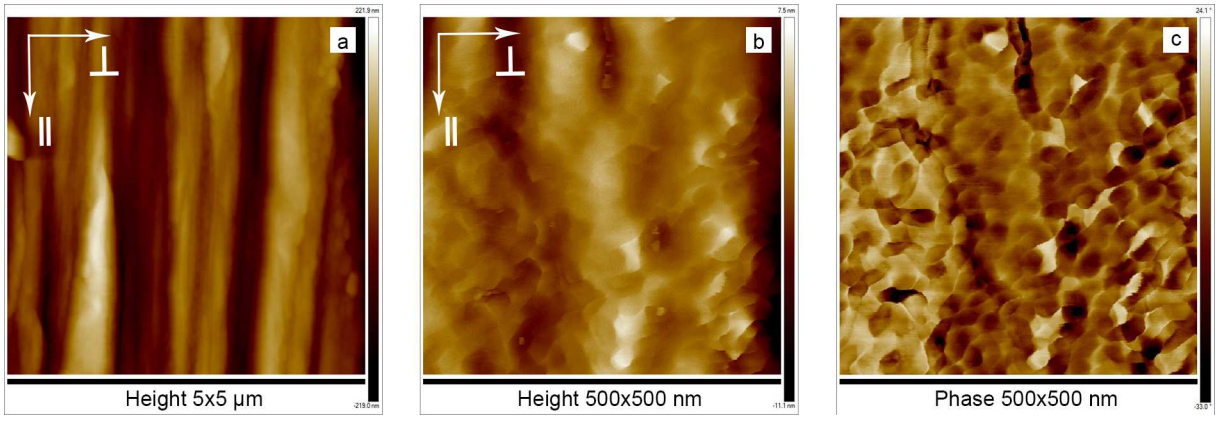

Figure 5. AFM height image (a) of 5x5 µm and height (b) and phase (c) image of 500x500 nm of PAN 3 after dissolving the finish.

Excerpt from ISBN 978-3-00-053387-7

3.3 BET investigations of the PAN fibers

To obtain information about the fiber surface averaged over a fiber tow, BET gas adsorption measurements were conducted. Based on literature, we expect surface values of $< 1\ m^2/g$. [25] Therefore, to increase the sensitivity, Krypton gas was chosen for the adsorption experiments. [26] The error of the BET measurements is $\pm\ 0.006\ m^2/g$. Table 2 shows the values of the BET specific surface area of the PAN fibers after desizing treatment. The technical fiber PAN 1 shows a larger specific surface area than PAN 2. The textile fiber PAN 3 shows the largest specific surface area. According to the investigation of the nanoroughness by AFM the specific surface area of PAN 1 and PAN 2 are expected to be similar. The difference in the BET specific surface area could be attributed to dominating influence of the fibril roughness. The fact, that the textile fiber PAN 3 shows the largest BET surface, is in agreement with AFM measurements.

Table 2. BET specific surface area.

Specimen Type	*BET surface* (m^2/g)
PAN 1	0.41
PAN 2	0.36
PAN 3	0.45

3.4 Crystal parameters of the three types of PAN fibers

Investigation of the fiber surface by AFM revealed a different degree of alignment of the pores along the fiber axis for the three PAN fiber types. We assume that these observation results from different degree of stretching during the fiber production process. Different degrees of stretching should be reflected in the PAN crystallite orientation. Therefore, the fibers were characterized by XRD, analyzing their crystallinity and crystallite orientation. The qualitative results of the XRD analysis are shown in Table 3.

Table 3. Relative degree of crystallinity and crystallite orientation of the three PAN fiber types**.**

Specimen Type	Crystallinity	Crystal Orientation
PAN 1	high	high
PAN 2	intermediate	intermediate
PAN 3	low	low

The three PAN fiber types show different crystallinity and different crystallite orientation. The crystallinity decreases in the following order: PAN 1 > PAN 2 > PAN 3. This result corresponds to the tensile strength of the resulting carbon fibers, which decreases in the same order. The orientation of the PAN crystallites also decreases in the same order: PAN 1 > PAN 2 > PAN 3. The result of this evaluation shows a correlation between the degree of orientation of pores obtained by AFM analysis and crystalline orientation. This suggests a correlation between the surface nanostructure and the crystalline order of the bulk material.

4. Conclusions

We have investigated the surface of three different types of PAN fibers on nanoscale by AFM. We used two technical fibers, which are precursors of carbon fibers, and a textile PAN fiber. The fibrils of all PAN fibers are oriented parallel to the fiber axis. A structure on nanoscale is detected for all PAN

Excerpt from ISBN 978-3-00-053387-7

fiber surfaces nanoporous in character. The nanopores vary in size and shape dependent on the fiber type. The two technical PAN fibers show similar size of the nanopores. However, the orientation of the pores along the fiber axis differes and increases with increasing tensile strength of the resulting carbon fiber. In contrast, the average pores size of the textile PAN fiber is larger and the orientation of the pores is less pronounced compared to the technical fibers. XRD measurements of the crystallinity and crystallite orientation correlate well with the surface nanostructure. The results show that the surface structure contains information about bulk properties of PAN fibers.

Acknowledgment

The authors express their sincere thanks to Gregor Schmidt-Bilkenroth and Ray Frenzel for XRD work.

References

[1] Olabisi, O. and Adewale, K. *Handbook of Thermoplastics*. CRC Press, Taylor & Francis Group, Boca Raton, 2016.

[2] Masson, J. C., Ed. *Acrylic fiber technology and applications*. M. Dekker, New York, 1995.

[3] Wilms, C., Seide, G. H., and Gries, T. The relationship between process technology, structure development and fibre properties in modern carbon fibre production. *Chemical Engineering Transactions*, 32:1609–1614, 2013.

[4] Paul, D. R. A study of spinnability in the wet-spinning of acrylic fibers. *Journal of Applied Polymer Science*, 12(10):2273–2298, 1968.

[5] Cahn, J. W. Phase Separation by Spinodal Decomposition in Isotropic Systems. *The Journal of Chemical Physics*, 42((1):93, 1965.

[6] Weisser, P., Barbier, G., Richard, C., and Drean, J.-Y. Characterization of the coagulation process. Wet-spinning tool development and void fraction evaluation. *Textile Research Journal*, 2015.

[7] Baojun, Q., Ding, P., and Zhenqiou, W. The mechanism and characterstics of dry-jet wet-spinning of acrylic fibers. *Advances in Polymer Technology*, 6(4):509–529, 1986.

[8] Arbab, S., Noorpanah, P., Mohammadi, N., and Soleimani, M. Designing index of void structure and tensile properties in wet-spun polyacrylonitrile (PAN) fiber. I. Effect of dope polymer or nonsolvent concentration. *Journal of Applied Polymer Science*, 109(6):3461–3469, 2008.

[9] van de Witte, P., Dijkstra, P. J., van den Berg, J., and Feijen, J. Phase separation processes in polymer solutions in relation to membrane formation. *Journal of Membrane Science*, 117(1-2):1–31, 1996.

[10] Cohen, C., Tanny, G. B., and Prager, S. Diffusion-controlled formation of porous structures in ternary polymer systems. *Journal of Polymer Science Part B-Polymer Physics*, 17(3):477–489, 1979.

[11] Knudsen, J. P. The Influence of Coagulation Variables on the Structure and Physical Properties of an Acrylic Fiber. *Textile Research Journal*, 33((1):13–20, 1963.

[12] Gupta, A. K., Paliwal, D. K., and Bajaj, P. Acrylic Precursors for Carbon Fibers. *Polymer Reviews*, 31((1):1–89, 1991.

[13] Frank, E., Hermanutz, F., and Buchmeiser, M. R. Carbon Fibers. Precursors, Manufacturing, and Properties. *Macromolecular Materials and Engineering*, 297(6):493–501, 2012.

Excerpt from ISBN 978-3-00-053387-7

[14] Frank, E., Steudle, L. M., Ingildeev, D., Spörl, J. M., and Buchmeiser, M. R. Carbon Fibers. Precursor Systems, Processing, Structure, and Properties. *Angewandte Chemie International Edition*, 53(21):5262–5298, 2014.

[15] Morita, K., Murata, Y., Ishitani, A., Murayama, K., Ono, T., and Nakajima, A. Characterization of commercially available PAN (polyacrylonitri1e)-based carbon fibers. *Pure and Applied Chemistry*, 58(3), 1986.

[16] Damodaran, S., Desai, P., and Abhiraman, A. S. Chemical and Physical Aspects of the Formation of Carbon Fibres from PAN-based Precursors. *The Journal of The Textile Institute*, 81(4):384–420, 2008.

[17] Chand, S. Review: Carbon fibers for composites. *Journal of Materials Science*, 35(6):1303–1313, 2000.

[18] Huang, X. Fabrication and Properties of Carbon Fibers. *Materials*, 2(4):2369–2403, 2009.

[19] Fitzer, E. Pan-based carbon fibers - present state and trend of the technology from the viewpoint of possibilities and limits to influence and to control the fiber properties by the process parameters. *Carbon*, 27(5):621–645, 1989.

[20] Magonov, S. N. and Reneker, D. H. Characterization of Polymer Surface with Atomic Force Microscopy. *Annual Review of Materials Science*, 27((1):175–222, 1997.

[21] Frenzel, R; Moosburger-Will, J; Horn, S. Evolution of crystalline parameters during stabilization of polyacrylontitrile fibers. *20th International Conference on Composite Materials, Copenhagen, Denmark*, July 19-24 2015.

[22] Kunzmann, C., Moosburger-Will, J., and Horn, S. High resolution imaging of the nanostructured surface of polyacrylonitrile-based fibers. *Journal of Materials Science*. submitted.

[23] Bajaj, P., Sreekumar, T. V., and Sen, K. Structure development during dry-jet-wet spinning of acrylonitrile/vinyl acids and acrylonitrile/methyl acrylate copolymers. *Journal of Applied Polymer Science*, 86(3):773–787, 2002.

[24] Bell, J. P. and Dumbleton, J. H. Changes in the Structure of Wet-Spun Acrylic Fibers During Processing. *Textile Research Journal*, 41(3):196–203, 1971.

[25] Jacobasch, H.-J. *Oberflächenchemie faserbildender Polymere. Akademie-Verlag*, 37, 1984.

[26] Yanazawa, H., Ohshika, K., and Matsuzawa, T. Precision Evaluation in Kr Adsorption for Small BET Surface Area Measurements of Less Than 1 m2. *Adsorption*, 6((1):73–77, 2000.

Excerpt from ISBN 978-3-00-053387-7